

## RESEARCH ARTICLE

Study of  $\alpha$ -Fe<sub>2</sub>O<sub>3</sub>@ZnO nanoleaves: Morphological and optical studyParastoo Khalili<sup>1</sup> Majid Farahmandjou<sup>2\*</sup>

**Abstract:** In this paper,  $\alpha$ -Fe<sub>2</sub>O<sub>3</sub>@ZnO nanoparticles (NPs) were synthesized by coprecipitation method in the presence of PVP and EG surfactants. The samples were characterized by x-ray fluorescence (XRF), x-ray diffraction (XRD), scanning electron microscopy (SEM), high resolution transmission electron microscopy (HRTEM), and fourier transform infrared spectroscopy (FTIR). The XRD results exhibited rhombohedral  $\alpha$ -Fe<sub>2</sub>O<sub>3</sub> and wurtzite structure of ZnO. The SEM images showed that the NPs changed from rod-shape to nanoleaves particles after heat treatment. The TEM studies displayed the formation of Fe<sub>2</sub>O<sub>3</sub>@ZnO core-shell of as-synthesized NPs. The stretching vibrations peaks in FTIR in the wavenumber of 532 cm<sup>-1</sup> and 473 cm<sup>-1</sup> ascribed to the Fe and Zn groups. The XRF data indicated decreasing of the Fe weight percent from 22% Wt. to 25% Wt., after heat treatment.

**Keywords:**  $\alpha$ -Fe<sub>2</sub>O<sub>3</sub>@ZnO, Nanoleaves, XRF, Crystal structure, FTIR

## 1 Introduction

Metal oxide semiconductors (MOS) are recognized as the best option for electronic and industry applications<sup>[1-5]</sup>. The MOS examples such as TiO<sub>2</sub><sup>[6-10]</sup>, CeO<sub>2</sub><sup>[11-14]</sup>, Fe<sub>2</sub>O<sub>3</sub><sup>[15-18]</sup>, ZnO<sup>[19-21]</sup>, Al<sub>2</sub>O<sub>3</sub><sup>[22-25]</sup>, V<sub>2</sub>O<sub>5</sub><sup>[26-30]</sup>, Co<sub>2</sub>O<sub>3</sub><sup>[31-33]</sup>, and composites such as FeCo<sup>[34-36]</sup> and FePt<sup>[37-39]</sup>, and coupled MOS such as Fe<sub>2</sub>O<sub>3</sub>-CeO<sub>2</sub><sup>[40-43]</sup>, SiO<sub>2</sub>-TiO<sub>2</sub><sup>[44]</sup>, Ce-doped Al<sub>2</sub>O<sub>3</sub><sup>[45,46]</sup>, Fe-doped Al<sub>2</sub>O<sub>3</sub><sup>[47-50]</sup>, Fe-doped TiO<sub>2</sub><sup>[51-54]</sup>, Ce-doped TiO<sub>2</sub><sup>[55-57]</sup>, Co-doped ZnO<sup>[58,59]</sup> are greatly used in optoelectronic applications and photocatalysts. However, study shows that the optical performance of MOS is limited due to rapid electron-hole recombination, light corrosion, and poor activity in sunlight. This factor has led scientists to do more research to improve the optical properties in visible light by reducing electron-hole recombination<sup>[60]</sup>. Among the various semiconductors application, zinc oxide (ZnO) has received much attention due to its unique structural, optical and surface properties. ZnO has a suitable bandgap about 3.73 eV and on the other hand its electron mobility is more than TiO<sub>2</sub>

with the same bandgap. The optical properties activity of ZnO is limited to the light radiation in the ultraviolet region due to its wide bandgap, and electron-hole recombination<sup>[61]</sup>. Fe<sub>2</sub>O<sub>3</sub> is also MOS that has been recognized as an important semiconductor which is active in visible light with a short band gap length of about 2.4 eV. In addition, iron oxide with magnetic properties has been proposed as an attractive idea for the separation of nanocatalysts from the liquid phase and has been studied in various photocatalytic processes of the liquid phase<sup>[62-64]</sup>. On the other hand, Fe<sub>2</sub>O<sub>3</sub> is able to send electrons into the wide band gap of MOS with a wide band gap like ZnO, which helps to reduce electron-hole recombination. Therefore, it can be expected that by activating the two ZnO and Fe<sub>2</sub>O<sub>3</sub> semiconductors, an active MOS in visible light will be achieved<sup>[65]</sup>. Fe<sub>2</sub>O<sub>3</sub>@ZnO coupled semiconductor increases the optical activity because of efficient electronhole separation at the interface. According to several investigations, Fe<sub>2</sub>O<sub>3</sub>@ZnO nanocomposites have been fabricated using various synthesis such as hydrothermal<sup>[66]</sup>, sol-gel<sup>[67]</sup>, solution combustion<sup>[68]</sup>, and emulsion<sup>[69]</sup> method. However, many of these methods suffer from several drawbacks such as long reaction time, requirement of high reaction temperature. Coprecipitation synthesis is regarded as a versatile tool for the synthesis of MOS NPs and is a simple and economic route to synthesize the Fe<sub>2</sub>O<sub>3</sub>@ZnO NPs<sup>[70]</sup>. Present study refers to the synthesis of Fe<sub>2</sub>O<sub>3</sub>@ZnO via a direct coprecipitation method and study the morphological and optical properties. The novelty of this work is the synthesis of Fe<sub>2</sub>O<sub>3</sub>@ZnO NPs with new precursors and solvent and study the new morphology of the fern-like Fe<sub>2</sub>O<sub>3</sub>@ZnO

Received: Sept. 27, 2020 Accepted: Oct. 18, 2020 Published: Oct. 20, 2020

\* Correspondence to: Majid Farahmandjou, Department of Chemistry, Faculty of Pharmaceutical Sciences, Tehran Medical Sciences, Islamic Azad University, Tehran, Iran; Email: farahmandjou@iautmu.ac.ir

<sup>1</sup> School of Architecture and Environmental Design, University of Science & Technology (IUST), Tehran, Iran

<sup>2</sup> Department of Chemistry, Faculty of Pharmaceutical Sciences, Tehran Medical Sciences, Islamic Azad University, Tehran, Iran

**Citation:** Khalili P and Farahmandjou M. Study of  $\alpha$ -Fe<sub>2</sub>O<sub>3</sub>@ZnO nanoleaves: Morphological and optical study. *Mater Eng Res*, 2020, 2(1): 118-124.

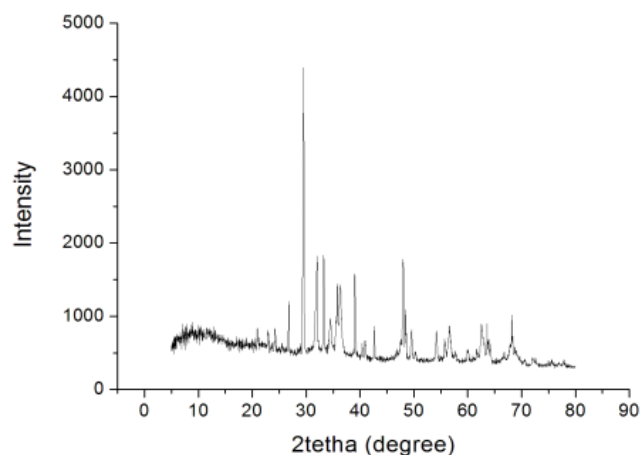
**Copyright:** © 2020 Parastoo Khalili, et al. This is an open access article distributed under the terms of the [Creative Commons Attribution License](https://creativecommons.org/licenses/by/4.0/), which permits unrestricted use, distribution, and reproduction in any medium, provided the original author and source are credited.

nanoleaves by changing the temperature.

## 2 Experimental details

$\alpha$ -Fe<sub>2</sub>O<sub>4</sub>@ZnO NPs were synthesized by coprecipitation method by iron nitrate (Fe(NO<sub>3</sub>)<sub>3</sub>·9H<sub>2</sub>O) and zinc nitrate (Zn(NO<sub>3</sub>)<sub>2</sub>·9H<sub>2</sub>O) precursors. At the beginning, 2 g iron nitrate was dissolved in 60 mL deionized water with stirring at room temperature. After 20 min, 2 g of zinc nitrate precursor was added to the solution and then 1 g of polyvinylpyrrolidone (PVP) stabilizer was added to the solution. After 5 min 10 mL ethylene glycol (EG) was slowly added to the solution. The temperature was increased to 90 °C and pH value of solution was measured about 4. The product were evaporated for 4 hours, cooled to room temperature and finally annealed at 650 °C for 3 hours. The specification of the size, structure and optical properties of the as-synthesis and annealed samples were carried out. XRD was used to identify the crystalline phase and to estimate the crystalline size. The XRD pattern were recorded with  $2\theta$  in the range of 4-85° with type X-Pert Pro MPD, Cu-K $\alpha$ :  $\lambda = 1.54 \text{ \AA}$ . The morphology of the samples was characterized by FESEM with type KYKY-EM3200, 25 kV and exact size of the NPs wa determined by TEM with type Zeiss EM-900, 80 kV. Stretching bound of the samples was characterized by FTIR with WQF 510. The elemental analysis of the NPs was carried out by Spectro Xepos ED-XRF spectroscopy.

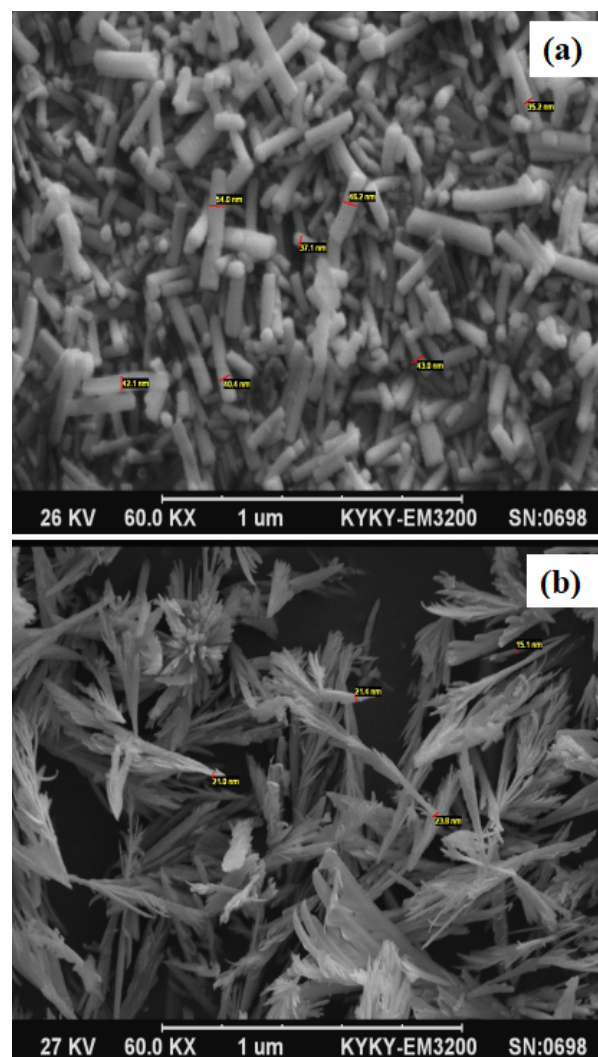
## 3 Results and discussion



**Figure 1.** XRD patterns of as-prepared and annealed Zinc ferrite samples

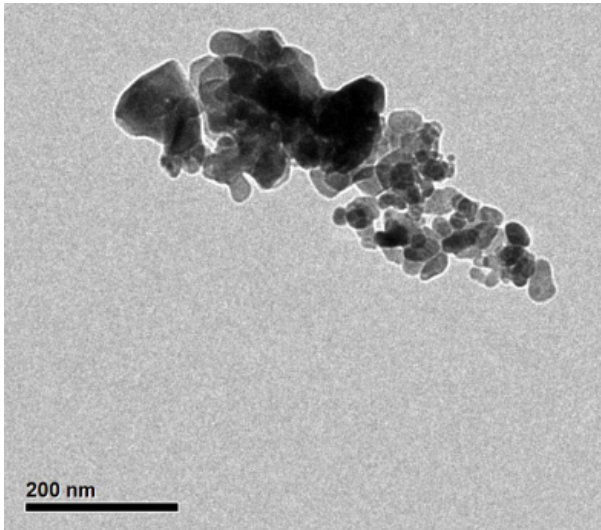
Figure 1 exhibits the XRD spectrum of the annealed  $\alpha$ -Fe<sub>2</sub>O<sub>4</sub>@ZnO NPs. The peaks correspond the  $\alpha$ -Fe<sub>2</sub>O<sub>3</sub> and ZnO NPs exhibit all the diffraction peaks of the hexagonal wurtzite ZnO and rhombohedral  $\alpha$ -Fe<sub>2</sub>O<sub>3</sub>, respectively. The peaks formed at  $2\theta$  angles of 31.98°,

35.73°, 36.28°, 47.98°, 56.55°, 62.49°, 66.33° and 68.17° are indexed the diffraction peaks at (100), (002), (101), (102), (110), (103), (200) and (112) respectively, represent the hexagonal wurtzite of zinc oxide. The peaks formed at 24.15°, 33.24°, 39.05°, 49.53°, 53.96°, 57.45°, and 63.60° which are correspond to the diffraction peaks at (012), (104), (113), (024), (300), (122), and (300) respectively, suggesting the rhombohedral  $\alpha$ -Fe<sub>2</sub>O<sub>3</sub> structure. Moreover, peaks formed at 26.46°, 29.46°, 42.60° and 54.14° indicating the  $\alpha$ -Fe<sub>2</sub>O<sub>3</sub>@ZnO structure. The crystallite size of the ordered  $\alpha$ -Fe<sub>2</sub>O<sub>3</sub>@ZnO samples have been calculated from full width at half maximum (FWHM) and Debye-Scherrer formula<sup>[71]</sup>. The crystallite size of the NPs are determined around 42 nm.

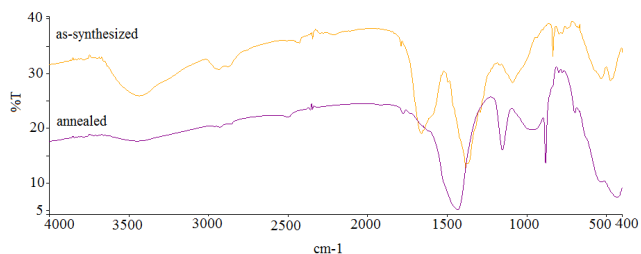


**Figure 2.** FESEM images of the (a) as-synthesized and (b) annealed samples

SEM analysis of the as-prepared and annealed  $\alpha$ -Fe<sub>2</sub>O<sub>3</sub>@ZnO samples was done to investigate the morphology of the samples. Figure 2(a) indicates the SEM



**Figure 3.** HRTEM image of the as-prepared Zinc ferrite sample



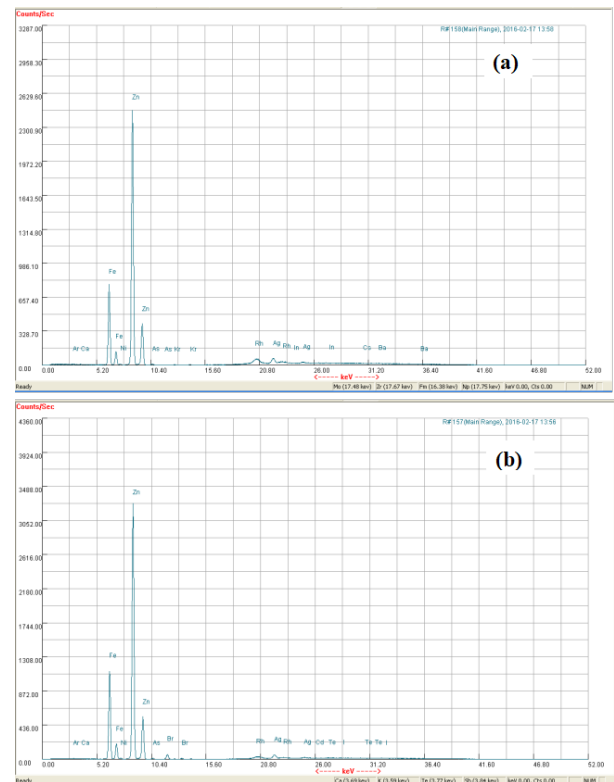
**Figure 4.** FTIR spectrum of (a) as-synthesized and (b) annealed  $\alpha$ -Fe<sub>2</sub>O<sub>3</sub>@ZnO samples

image of the as-prepared samples and [Figure 2\(b\)](#) shows the SEM image of the annealed NPs at 650 °C for 3 hours. The morphology of the samples show that the samples change from rod-shape to fern-like Fe<sub>2</sub>O<sub>3</sub>@ZnO nanoleaves after heat treatment<sup>[70]</sup>. In fact, the PVP and EG stabilizers are removed by annealing process and the atomic and molecular interactions change between particles that lead the fern-like nanoleaves formation<sup>[72–77]</sup>.

In order to measure the actual size of the NPs the TEM analysis was done [Figure 3](#) shows the as-prepared TEM image of  $\alpha$ -Fe<sub>2</sub>O<sub>3</sub>@ZnO core-shell nanoparticles with average diameter of 48 nm prepared by coprecipitation method which is in accordance with XRD analysis<sup>[78–81]</sup>. From the TEM, Fe<sub>2</sub>O<sub>3</sub> particles are formed as nuclei magnetic and zinc oxide as the shell of these NPs. It can be seen from TEM image, the core-shell formation lead to the aggregation and agglomeration of the NPs.

[Figure 4](#) shows the FTIR spectra of the as-synthesized and annealed  $\alpha$ -Fe<sub>2</sub>O<sub>3</sub>@ZnO NPs in the range of 400–4000 cm<sup>-1</sup> frequencies to identify the chemical bonds as well as functional groups in the compound. The large broad band at 3436 cm<sup>-1</sup> is attributed to the O-H stretching groups. The spectra of the annealed sample demonstrates that the O-H band reduces and it shifts to higher

energy values at 3459 cm<sup>-1</sup> which shows that O-H groups are chemically bonded to the oxide structure<sup>[82]</sup>. The sharp peaks at 1662 cm<sup>-1</sup> and 1384 cm<sup>-1</sup> are due to bending vibration of C = O respectively. The peaks in the frequencies of 532 cm<sup>-1</sup> and 473 cm<sup>-1</sup> are assigned to the stretching vibrations of Zn-O and Fe-O bonds<sup>[83,84]</sup>.



**Figure 5.** XRF analysis of (a) as-prepared and (b) annealed Zinc ferrite NPs

XRF analysis of  $\alpha$ -Fe<sub>2</sub>O<sub>3</sub>@ZnO samples prepared by coprecipitation method is presented in [Figure 5](#). The as-synthesized and annealed samples confirms the existence of Zn and Fe elements. XRF exhibits the peaks of Fe and Zn elements with less Pb, Sb, Bi and Sn contaminations. The XRF data revealed increasing of the Fe weight percent from 22% Wt. to 25% Wt., by annealing. It may be because of increasing of the Fe<sup>3+</sup> into the crystal lattice. The value of Fe<sup>3+</sup>/ZnO is obtained 0.28 for the as-prepared NPs, while it is achieved 0.32 for the annealed samples suggesting an increase in the Fe content.

## 4 Conclusion

$\alpha$ -Fe<sub>2</sub>O<sub>3</sub>@ZnO NPs were successfully fabricated by simple coprecipitation method. The XRD spectra exhibited the rhombohedral  $\alpha$ -Fe<sub>2</sub>O<sub>3</sub> structure and wurtzite ZnO structure. The SEM images indicated that the NPs changed from rod-shape to fern-like Fe<sub>2</sub>O<sub>3</sub>@ZnO

nanoleaves after heat treatment. TEM image showed the formation of core-shell  $\alpha$ -Fe<sub>2</sub>O<sub>3</sub>@ZnO NPs. FTIR analysis ascribed the presence of Fe and Zn stretching bound and it also confirmed the formation of  $\alpha$ -Fe<sub>2</sub>O<sub>3</sub>@ZnO bound. Finally, the XRF analysis demonstrated an increase in Fe content into the crystal lattice.

## Acknowledgements

The authors are thankful for the financial support of varamin pishva branch at Islamic Azad University for analysis and the discussions on the results.

## References

- [1] Moghimi A and Farahmandjou M. Preconcentration of Cd (II) by chemically converted graphene sheets adsorbed on surfactant-coated C18 before determination by flame atomic absorption spectrometry (FAAS). *African Journal of Pure and Applied Chemistry*, 2014, **8**(1): 1-8. <https://doi.org/10.5897/AJPAC2013.0542>
- [2] Farahmandjou M. Liquid Phase Synthesis of indium tin oxide (ITO) nanoparticles using In (III) and Sn (IV) salts. *Australian Journal of Basic and Applied Sciences*, 2013, **7**(4): 31-34.
- [3] Farahmandjou M. Synthesis of ITO Nanoparticles Prepared by Degradation of Sulfide Method. *Chinese Physics Letters*, 2012, **29**, 077306-9. <https://doi.org/10.1088/0256-307X/29/7/077306>
- [4] Farahmandjou M. The study of electro-optical properties of nanocomposite ITO thin films prepared by e-beam evaporation. *Revista mexicana de fsica*, 2013, **59**: 205-207.
- [5] Farahmandjou M. Synthesis and Morphology Study of Nano-Indium Tin Oxide (ITO) Grains. *International Journal of Bio-Inorganic Hybrid Nanomaterials*, 2013, **2**(2): 373.
- [6] Farahmandjou M and Ramazani M. Fabrication and Characterization of Rutile TiO<sub>2</sub> Nanocrystals by Water Soluble Precursor. *Physical Chemistry Research*, 2015, **3**: 293-298. <https://doi.org/10.22036/pcr.2015.10641>
- [7] Farahmandjou M and Khalili P. Morphology Study of anatase nano-TiO<sub>2</sub> for Self-cleaning Coating. *International Journal of Physical Sciences*, 2013, **3**: 54-56. <https://doi.org/10.14331/ijfps.2013.330055>
- [8] Farahmandjou M. One-step synthesis of TiO<sub>2</sub> nanoparticles using simple chemical technique. *Materials Science and Engineering*, 2019, **1**(1): 15-19. <https://doi.org/10.25082/MER.2019.01.004>
- [9] Ramazani M, Farahmandjou M and Firoozabadi TP. Effect of nitric acid on particle morphology of the nano-TiO<sub>2</sub>. *International Journal of Nanoscience and Nanotechnology*, 2015, **11**: 115-122.
- [10] Farahmandjou M. Self-cleaning measurement of nano-sized photoactive TiO<sub>2</sub>. *Journal of Computer and Robotics*, 2014, **7**(2): 15-19.
- [11] Zarinkamar M, Farahmandjou M and Firoozabadi TP. Diethylene Glycol-Mediated Synthesis of Nano-Sized Ceria (CeO<sub>2</sub>) Catalyst. *Journal of Nanostructures*, 2016, **6**: 116-120. <https://doi.org/10.7508/jns.2016.02.002>
- [12] Zarinkamar M, Farahmandjou M and Firoozabadi TP. One-step synthesis of ceria (CeO<sub>2</sub>) nano-spheres by a simple wet chemical method. *Journal of Ceramic Processing Research*, 2016, **17**: 166-169.
- [13] Farahmandjou M and Zarinkamar M. Synthesis of nano-sized ceria (CeO<sub>2</sub>) particles via a cerium hydroxy carbonate precursor and the effect of reaction temperature on particle morphology. *Journal of Ultrafine Grained and Nanostructured Materials*, 2015, **48**: 5-10. <https://doi.org/10.7508/jufngsm.2015.01.002>
- [14] Farahmandjou M, Zarinkamar M and Firoozabadi TP. Synthesis of Cerium Oxide (CeO<sub>2</sub>) nanoparticles using simple Co-precipitation method. *Revista Mexicana de Fsica*, 2016, **62**: 496-499.
- [15] Farahmandjou M and Soflaee F. Synthesis and characterization of  $\alpha$ -Fe<sub>2</sub>O<sub>3</sub> nanoparticles by simple co-precipitation method. *Physical Chemistry Research*, 2015, **3**: 193-198. <https://doi.org/10.22036/pcr.2015.9193>
- [16] Farahmandjou M and Soflaee F. Polymer-Mediated Synthesis of Iron Oxide (Fe<sub>2</sub>O<sub>3</sub>) Nanorods. *Chinese Journal of Physics*, 2015, **53**: 080801-9. <https://doi.org/10.6122/CJP.20150413>
- [17] Farahmandjou M and Soflaee F. Low Temperature Synthesis of  $\alpha$ -Fe<sub>2</sub>O<sub>3</sub> Nano-rods Using Simple Chemical Route. *Journal of Nanostructures*, 2014, **4**(4): 413-418. <https://doi.org/10.7508/jns.2014.04.002>
- [18] Farahmandjou M and Soflaee F. Synthesis of Iron Oxide Nanoparticles using Borohydride Reduction. *International Journal of Bio-Inorganic Hybrid Nanomaterials*, 2014, **3**: 203-206.
- [19] Jurablu S, Farahmandjou M and Firoozabadi TP. Multiple-layered structure of obelisk-shaped crystalline nano-ZnO prepared by sol-gel route. *Journal of Theoretical and Applied Physics*, 2015, **9**: 261-266. <https://doi.org/10.1007/s40094-015-0184-6>
- [20] Jurablu S, Farahmandjou M and Firoozabadi TP. Sol-gel synthesis of zinc oxide (ZnO) nanoparticles: study of structural and optical properties. *Journal of Sciences, Islamic Republic of Iran*, 2015, **26**: 281-285.
- [21] Farahmandjou M and Jurablu S. Co-precipitation Synthesis of Zinc Oxide (ZnO) Nanoparticles by Zinc Nitrate Precursor. *International Journal of Bio-Inorganic Hybrid Nanomaterials*, 2014, **3** (3): 179-184.
- [22] Farahmandjou M and Golabiyani N. Synthesis and characterization of Alumina (Al<sub>2</sub>O<sub>3</sub>) nanoparticles prepared by simple sol-gel method. *International Journal of Bio-Inorganic Hybrid Nanomaterials*, 2016, **5**(1): 73-77.
- [23] Farahmandjou M and Golabiyani N. Solution combustion preparation of nano-Al<sub>2</sub>O<sub>3</sub>: Synthesis and characterization. *Transport Phenomena in Nano and Micro Scales*, 2015, **3**: 100-105. <https://doi.org/10.7508/tpnms.2015.02.004>
- [24] Farahmandjou M and Golabiyani N. New pore structure of nano-alumina (Al<sub>2</sub>O<sub>3</sub>) prepared by sol gel method. *Journal of Ceramic Processing Research*, 2015, **16**(2): 1-4.

- [25] Farahmandjou M and Golabiyani N. Synthesis and characterisation of  $\text{Al}_2\text{O}_3$  nanoparticles as catalyst prepared by polymer co-precipitation method. *Materials Science and Engineering*, 2019, **1**(2): 40-44.  
<https://doi.org/10.25082/MER.2019.02.002>
- [26] Farahmandjou M and Salehizadeh SA. The optical band gap and the tailing states determination in glasses of  $\text{TeO}_2$ - $\text{V}_2\text{O}_5$ - $\text{K}_2\text{O}$  system. *Glass Physics and Chemistry*, 2013, **39**: 473-479.  
<https://doi.org/10.1134/S1087659613050052>
- [27] Farahmandjou M and Abaeian N. Simple Synthesis of Vanadium Oxide ( $\text{V}_2\text{O}_5$ ) Nanorods in Presence of CTAB Surfactant. *Colloid Surface Science*, 2016, **1**: 10-13.  
<https://doi.org/10.15406/jnmr.2017.05.00103>
- [28] Farahmandjou M and Salehizadeh SA. Investigation on calorimetric and elastic properties of  $50\text{TeO}_2$ - $(50-x)\text{V}_2\text{O}_5$ - $x\text{K}_2\text{O}$  glassy systems. *Chalcogenide Letters*, 2015, **12** (11): 619-631.  
<https://doi.org/10.1016/j.jnoncrysol.2016.03.012>
- [29] Farahmandjou M and N Abaeiyan. Chemical synthesis of vanadium oxide ( $\text{V}_2\text{O}_5$ ) nanoparticles prepared by sodium metavanadate. *Journal of Nanomedicine Research*, 2017, **5**(1): 00103.  
<https://doi.org/10.15406/jnmr.2017.05.00103>
- [30] Farahmandjou M and Abaeiyan N. Simple synthesis of new nano-sized pore structure vanadium pentoxide ( $\text{V}_2\text{O}_5$ ). *International Journal of Bio-Inorganic Hybrid Nanomaterials*, 2015, **4**(4): 243-247.
- [31] Shadrokh S, Farahmandjou M and Firozabadi TP. Fabrication and Characterization of Nanoporous Co Oxide ( $\text{Co}_3\text{O}_4$ ) Prepared by Simple Sol-gel Synthesis. *Physical Chemistry Research*, 2016, **4**: 153-160.  
<https://doi.org/10.22036/pcr.2016.12909>
- [32] Farahmandjou M and Shadrokh S. Chemical synthesis of the  $\text{Co}_3\text{O}_4$  nanoparticles in presence of CTAB surfactant. *International Journal of Bio-Inorganic Hybrid Nanomaterials*, 2015, **4**(3): 129-134.
- [33] Farahmandjou M. Preparation of Ferromagnetic  $\text{Co}_3\text{O}_4$  Nanoparticles by Wet Chemical Synthesis Method. *To Physics Journal*, 2019, **3**: 89-99.
- [34] Honarbakhsh S, Farahmandjou M and Behroozinia S. Synthesis and characterization of iron cobalt (FeCo) nanorods prepared by simple Co-precipitation method. *Journal of Fundamental and Applied Sciences*, 2016, **8**: 892-900.  
<https://doi.org/10.4314/jfas.8vi2s.142>
- [35] Farahmandjou M, Honarbakhsh S and Behrouziniya S. FeCo Nanorods Preparation Using New Chemical Synthesis. *Journal of Superconductivity and Novel Magnetism*, 2018, **31**: 4147-4152.  
<https://doi.org/10.1007/s10948-018-4659-y>
- [36] Farahmandjou M, Honarbakhsh S and Behrouziniya S. PVP-Assisted Synthesis of Cobalt Ferrite ( $\text{CoFe}_2\text{O}_4$ ) Nanorods. *Physical Chemistry Research*, 2016, **4**: 655-662.  
<https://doi.org/10.22036/pcr.2016.16702>
- [37] Farahmandjou M. Synthesis and Structural Study of L10-FePt NPs. *Turkish Journal of Engineering and Environmental Sciences*, 2010, **34**: 265-270.  
<https://doi.org/10.3906/muh-1010-20>
- [38] Farahmandjou M. Magnetocrystalline properties of Iron-Platinum (L10-FePt) nanoparticles through phase transition. *Iranian Journal of Physics Research*, 2016, **16**: 1-5.  
<https://doi.org/10.18869/acadpub.ijpr.16.1.1>
- [39] Farahmandjou M. Effect of Oleic Acid and Oleylamine Surfactants on the Size of FePt Nanoparticles. *Journal of Superconductivity and Novel Magnetism*, 2012, **25**: 2075-2079.  
<https://doi.org/10.1007/s10948-012-1586-1>
- [40] Dastpak M, Farahmandjou M and Firoozabadi TP. Synthesis and Preparation of Magnetic Fe-Doped  $\text{CeO}_2$  Nanoparticles Prepared by Simple Sol-Gel Method. *Journal of Superconductivity and Novel Magnetism*, 2016, **29**: 2925-2929.  
<https://doi.org/10.1007/s10948-016-3639-3>
- [41] Farahmandjou M and Dastpak M. Fe-Loaded  $\text{CeO}_2$  Nanosized Prepared by Simple Co-Precipitation Route. *Physical Chemistry Research*, 2018, **6**: 713-720.
- [42] Farahmandjou M and Dastpak M. Synthesis of Fe-doped  $\text{CeO}_2$  Nanoparticles Prepared by Solgel Method. *Journal of Sciences, Islamic Republic of Iran*, 2020, **31**(1): 39-43.  
<https://doi.org/10.22059/jsciences.2020.256813.1007255>
- [43] Farahmandjou M, Dastpak M and Panji Z. CTAB-assisted of  $\text{Fe}_2\text{O}_3/\text{CeO}_2$  nanosized prepared by coprecipitation method. *International Journal of Bio-Inorganic Hybrid Nanomaterials*, 2018, **7**(3): 221-226.
- [44] Farahmandjou M and Khalili P. Study of Nano  $\text{SiO}_2/\text{TiO}_2$  Superhydrophobic Self-Cleaning Surface Produced by Sol-Gel. *Australian Journal of Basic and Applied Sciences*, 2013, **7**: 462-465.
- [45] Motaghi S and Farahmandjou M. Structural and optoelectronic properties of Ce- $\text{Al}_2\text{O}_3$  nanoparticles prepared by sol-gel precursors. *Materials Research Express*, 2019, **6**: 045008.  
<https://doi.org/10.1088/2053-1591/aaf927>
- [46] Farahmandjou M and Motaghi S. Sol-gel Synthesis of Ce-doped  $\alpha$ - $\text{Al}_2\text{O}_3$ : Study of Crystal and Optoelectronic Properties. *Optics Communications*, 2019, **441**: 1-7.  
<https://doi.org/10.1016/j.optcom.2019.02.029>
- [47] Khodadadi A, Farahmandjou M, Yaghoubi M, *et al.* Structural and Optical Study of  $\text{Fe}^{3+}$ -Doped  $\text{Al}_2\text{O}_3$  Nanocrystals Prepared by New Sol gel Precursors. *International Journal of Applied Ceramic Technology*, 2018, **16**: 718-726.  
<https://doi.org/10.1111/ijac.13065>
- [48] Khodadadi A, Farahmandjou M and Yaghoubi M. Investigation on synthesis and characterization of Fe-doped  $\text{Al}_2\text{O}_3$  nanocrystals by new sol-gel precursors. *Materials Research Express*, 2019, **6**: 025029.  
<https://doi.org/10.1088/2053-1591/aaef70>
- [49] Farahmandjou M, Khodadadi A and Yaghoubi M. Synthesis and Characterization of Fe- $\text{Al}_2\text{O}_3$  nanoparticles Prepared by Coprecipitation Method. *Iranian Journal of Chemistry and Chemical Engineering (IJCCE)*, in press.  
<https://doi.org/10.30492/ijcce.2020.38036>
- [50] Farahmandjou M, Khodadadi A and Yaghoubi M. Low Concentration Iron-Doped Alumina ( $\text{Fe}/\text{Al}_2\text{O}_3$ ) Nanoparticles Using Co-Precipitation Method. *Journal of Superconductivity and Novel Magnetism*, 2020.  
<https://doi.org/10.1007/s10948-020-05569-0>
- [51] Farahmandjou M and Behrouziniya S. Fe Lauded  $\text{TiO}_2$  Nanoparticles Synthesized by Sol-gel Precursors. *Physical Chemistry Research*, 2019, **7**(2): 395-401.  
<https://doi.org/10.22036/pcr.2019.151365.1546>

- [52] Khoshnevisan B, Marami MB and Farahmandjou M. Fe<sup>3+</sup>-Doped Anatase TiO<sub>2</sub> Study Prepared by New Sol-Gel Precursors. *Chinese Physics Letters*, 2018, **35**: 027501-5. <https://doi.org/10.1088/0256-307X/35/2/027501>
- [53] Marami MB, Farahmandjou M and Khoshnevisan B. Sol-gel Synthesis of Fe-doped TiO<sub>2</sub> Nanocrystals. *Journal of Electronic Materials*, 2018, **47**: 3741-3749. <https://doi.org/10.1007/s11664-018-6234-5>
- [54] Jafari A, Khademi S, Farahmandjou M, et al. Preparation and Characterization of Cerium Doped Titanium Dioxide Nanoparticles by the Electrical Discharge Method. *Journal of Advanced Materials in Engineering*, 2019, **38**(2): 83-90. <https://doi.org/10.29252/jame.38.2.83>
- [55] Jafari A, Khademi S and Farahmandjou M. Nano-crystalline Ce-doped TiO<sub>2</sub> Powders: Sol-gel Synthesis and Optoelectronic Properties. *Materials Research Express*, 2018, **5**(9): 095008. <https://doi.org/10.1088/2053-1591/aad5b5>
- [56] Jafari A, Khademi S, Farahmandjou M, et al. Structural and optical properties of Ce<sup>3+</sup>-doped TiO<sub>2</sub> nanocrystals prepared by sol-gel precursors. *Journal of Electronic Materials*, 2018, **47**: 6901-6908. <https://doi.org/10.1007/s11664-018-6590-1>
- [57] Marami MB and Farahmandjou M. Water-Based Sol-Gel Synthesis of Ce-Doped TiO<sub>2</sub> Nanoparticles. *Journal of Electronic Materials*, 2019, **48**: 4740-4747. <https://doi.org/10.1007/s11664-019-07265-9>
- [58] Akhtari F, Zorriasatein S, Farahmandjou M, et al. Structural, optical, thermoelectrical, and magnetic study of Zn<sub>1-x</sub>CoxO (0 ≤ x ≤ 0.10) nanocrystals. *International Journal of Applied Ceramic Technology*, 2018, **15**: 723-733. <https://doi.org/10.1111/ijac.12848>
- [59] Akhtari F, Zorriasatein S, Farahmandjou M, et al. Synthesis and optical properties of Co<sup>2+</sup>-doped ZnO Network prepared by new precursors. *Materials Research Express*, 2018, **5**: 065015. <https://doi.org/10.1088/2053-1591/aac6f1>
- [60] Ehsana MF and Hea T. In situ synthesis of ZnO/ZnTe common cation hetero structure and its visible-light photocatalytic reduction of CO<sub>2</sub> in to CH<sub>4</sub>. *Applied Catalysis B: Environmental*, 2015, **166-167**: 345-352. <https://doi.org/10.1016/j.apcatb.2014.11.058>
- [61] Xie J, Zhou Z, Lian Y, et al. Synthesis of  $\alpha$ -Fe<sub>2</sub>O<sub>3</sub>/ZnO composites for photocatalytic degradation of pentachlorophenol under UV-vis light irradiation. *Ceramics International*, 2015, **41**: 2622-2625. <https://doi.org/10.1016/j.ceramint.2014.10.043>
- [62] Achouri F, Corbel S, Aboulaich A, et al. Aqueous synthesis and enhanced photocatalytic activity of ZnO/Fe<sub>2</sub>O<sub>3</sub> heterostructures. *Journal of Physics and Chemistry of Solids*, 2014, **75**: 1081-108. <https://doi.org/10.1016/j.jpcc.2014.05.013>
- [63] Vijay Kumar S, Huang NM, Yusoff N, et al. High performance magnetically separable graphene/ zinc oxide nanocomposite. *Materials Letters*, 2013, **93**: 411-414. <https://doi.org/10.1016/j.matlet.2012.09.089>
- [64] Liu Y, Sun L, Wu J, et al. Preparation and photocatalytic activity of ZnO/Fe<sub>2</sub>O<sub>3</sub> nanotube composites. *Materials Science and Engineering: B*, 2015, **194**: 9-13. <https://doi.org/10.1016/j.mseb.2014.12.021>
- [65] Yin Q, Qiaon R, Zhu L, et al.  $\alpha$ -Fe<sub>2</sub>O<sub>3</sub> decorated ZnO nanorod-assembled hollow microspheres: Synthesis and enhanced visible-light photocatalysis. *Materials Letters*, 2014, **135**: 135-138. <https://doi.org/10.1016/j.matlet.2014.07.149>
- [66] Dem'Yanets LN, Li LE and Uvarova TG. Zinc oxide: hydrothermal growth of nanoand bulk crystals and their luminescent properties. *Journal of Materials Science*, 2006, **41**(5): 1439-1444. <https://doi.org/10.1007/s10853-006-7457-z>
- [67] Risti M, Musi S, Ivanda M, et al. Sol-gel synthesis and characterization of nanocrystalline ZnO powders. *Journal of Alloys and Compounds*, 2005, **397**(1-2): L1-L4. <https://doi.org/10.1016/j.jallcom.2005.01.045>
- [68] Zulfiqar Ahmed MN, Chandrasekhar KB, Jahagirdar AA, et al. Photocatalytic activity of nanocrystalline ZnO,  $\alpha$ -Fe<sub>2</sub>O<sub>3</sub> and ZnFe<sub>2</sub>O<sub>4</sub>/ZnO. *Applied Nanoscience*, 2015, **5**: 961-968. <https://doi.org/10.1007/s13204-014-0395-1>
- [69] Radzimska AK, Markiewicz E and Jesionowski T. Structural characterization of ZnO particles obtained by the emulsion precipitation method. *Journal of Nanomaterials*, 2012. 656353. <https://doi.org/10.1155/2012/656353>
- [70] Hoseini F, Farahmandjou M and Firoozabadi TP. Coprecipitation synthesis of zinc ferrite (Fe<sub>2</sub>O<sub>3</sub>/ZnO) nanoparticles prepared by CTAB surfactant. *Journal of Fundamental and Applied Sciences*, 2016, **8**(3S): 738-745. <https://doi.org/10.4314/jfas.v8i3s.258>
- [71] Scherrer P. Bestimmung der Grosse und der Inneren Struktur von Kolloidteilchen Mittels Rontgenstrahlen, *Nachrichten von der Gesellschaft der Wissenschaften. Göttingen. Mathematisch-Physikalische Klasse*, 1918, **2**: 98-100. <https://doi.org/10.4236/health.2011.370702,486>
- [72] Sebt SA, Parhizgar SS, Farahmandjou M, et al. The role of ligands in the synthesis of FePt nanoparticles. *Journal of Superconductivity and Novel Magnetism*, 2009, **22**: 849-854. <https://doi.org/10.1007/s10948-009-0509-2>
- [73] Farahmandjou M, Sebt SA, Parhizgar SS, et al. Stability investigation of colloidal FePt nanoparticle systems by spectrophotometer analysis. *Chinese Physics Letters*, 2009, **26**: 027501-3. <https://doi.org/10.1088/0256-307X/26/2/027501>
- [74] Farahmandjou M, Sebt SA, Parhizgar SS, et al. The Effect of NaCl Prepared by Ultra-sonic Vibration on the Sintering of Annealed FePt Nanoparticles. *Journal of Physics: Conference Series*, **153**(1): 012050. <https://doi.org/10.1088/1742-6596/153/1/012050>
- [75] Farahmandjou M. Comparison of the Fe and Pt nanoparticles with FePt alloy prepared by polyol process: Shape and composition study. *Acta Physica Polonica A*, 2013, **123**: 277-278. <https://doi.org/10.12693/APhysPolA.123.277>
- [76] Behrouzinia S, Salehinia D, Khorasani K, et al. The continuous control of output power of a CuBr laser by a pulsed external magnetic field. *Optics Communications*, 2019, **436**: 143-145. <https://doi.org/10.1016/j.optcom.2018.12.016>

- [77] Behrouzinia S, Khorasani K and Farahmandjou M. Buffer gas effects on output power of a copper vapor laser. *Laser Physics*, 2016, **26**(5): 055003.  
<https://doi.org/10.1088/1054-660X/26/5/055003>
- [78] Farahmandjou M. The effect of reflux process on the size and uniformity of FePt nanoparticles. *International Journal of fundamental physical sciences*, 2011, **1**(3): 57-59.  
<https://doi.org/10.14331/ijfps.2011.330014>
- [79] Farahmandjou M. Two step growth process of iron-platinum (FePt) nanoparticles. *International Journal of Physical Sciences*, 2012, **7**(19): 2713-2719.  
<https://doi.org/10.5897/IJPS11.1456>
- [80] Farahmandjou M. Shape and composition study of iron-platinum (FePt) nanoalloy prepared by polyol process. *International Journal of Physical Sciences*, 2012, **7**(12): 1938-1942.  
<https://doi.org/10.5897/IJPS11.1710>
- [81] Farahmandjou M. The Effect of 1, 2-Hexadecadienol and LiBEt<sub>3</sub>H Superhydride on the Size of FePt Nanoparticles. *AIP Conference Proceedings*, 2011, **1415**(1): 193-195.  
<https://doi.org/10.1063/1.3667254>
- [82] Nakamoto K. *Infrared and raman spectra of inorganic and coordination compounds*. John Wiley and Sons, 1978.
- [83] Ferraro JR. *Low frequency vibrations of inorganic and coordination compounds*. Plenum Press, New York, 1971.  
[https://doi.org/10.1007/978-1-4684-1809-5\\_9](https://doi.org/10.1007/978-1-4684-1809-5_9)
- [84] Lopez T, Mendez J, Zamudio T, *et al.* *Materials Chemistry and Physics*, 1992, **30**: 161-167.  
[https://doi.org/10.1016/0254-0584\(92\)90218-W](https://doi.org/10.1016/0254-0584(92)90218-W)